THE JOURNAL OF BIOLOGICAL CHEMISTRY VOL. 290, NO. 17, pp. 10934–10946, April 24, 2015

Chronic Deletion and Acute Knockdown of Parkin Have Differential Responses to Acetaminophen-induced Mitophagy and Liver Injury in Mice*

Received for publication, August 4, 2014, and in revised form, February 25, 2015 Published, JBC Papers in Press, March 9, 2015, DOI 10.1074/jbc.M114.602284

Jessica A. Williams, Hong-Min Ni, Anna Haynes, Sharon Manley, Yuan Li, Hartmut Jaeschke, and Wen-Xing Ding[1]

From the Department of Pharmacology, Toxicology and Therapeutics, University of Kansas Medical Center, Kansas City, Kansas 66160

Background: Parkin is required for mitophagy in cultured cells, but its role in liver injury is not known.
Results: APAP-induced mitophagy was impaired in acute Parkin knockdown mouse livers but not whole body Parkin knock-out mice.
Conclusion: Chronic, but not acute, loss of Parkin protects against APAP-induced liver injury by multiple mechanisms independent of mitophagy.
Significance: This study revealed a novel role of Parkin in APAP-induced liver injury.

We previously demonstrated that pharmacological induction of autophagy protected against acetaminophen (APAP)-induced liver injury in mice by clearing damaged mitochondria. However, the mechanism for removal of mitochondria by autophagy is unknown. Parkin, an E3 ubiquitin ligase, has been shown to be required for mitophagy induction in cultured mammalian cells following mitochondrial depolarization, but its role *in vivo* is not clear. The purpose of this study was to investigate the role of Parkin-mediated mitophagy in protection against APAP-induced liver injury. We found that Parkin translocated to mitochondria in mouse livers after APAP treatment followed by mitochondrial protein ubiquitination and mitophagy induction. To our surprise, we found that mitophagy still occurred in Parkin knock-out (KO) mice after APAP treatment based on electron microscopy analysis and Western blot analysis for some mitochondrial proteins, and Parkin KO mice were protected against APAP-induced liver injury compared with wild type mice. Mechanistically, we found that Parkin KO mice had decreased activated c-Jun N-terminal kinase (JNK), increased induction of myeloid leukemia cell differentiation protein (Mcl-1) expression, and increased hepatocyte proliferation after APAP treatment in their livers compared with WT mice. In contrast to chronic deletion of Parkin, acute knockdown of Parkin in mouse livers using adenovirus shRNA reduced mitophagy and Mcl-1 expression but increased JNK activation after APAP administration, which exacerbated APAP-induced liver injury. Therefore, chronic deletion (KO) and acute knockdown of Parkin have differential responses to APAP-induced mitophagy and liver injury in mice.

Acetaminophen (APAP)[2] overdose is the main cause of acute liver failure in the United States and can even lead to death (1). APAP is metabolized by cytochrome P450s, mainly by Cyp2e1, to the reactive metabolite NAPQI (*N*-acetyl-*p*-benzoquinone imine), which is bound and detoxified by glutathione (GSH) after therapeutic doses of APAP. APAP overdose causes GSH depletion and allows for NAPQI to bind to proteins, which leads to mitochondrial dysfunction and hepatocyte necrosis (2). We previously found that pharmacological induction of autophagy via rapamycin was protective against APAP-induced liver injury, likely by removing damaged mitochondria (3, 4). However, the mechanism for removal of these damaged mitochondria in the liver is unknown.

Macroautophagy (hereafter referred to as autophagy) is an evolutionarily conserved process that results in degradation of cellular proteins and organelles due to a cell's "self-eating." In addition to providing the cell with nutrients and energy in response to starvation, this process rids the cell of misfolded proteins and damaged organelles through the formation of double-membrane autophagosomes. Autophagosomes can engulf individual organelles, protein aggregates, or portions of cytoplasm before fusing with lysosomes to degrade their contents (5). Autophagy is a protective process that can be either selective or nonselective. Nonselective autophagy occurs during starvation to break down the cell's components to provide a source of energy and nutrients. Selective autophagy occurs in nutrient-rich or -poor conditions as a protective mechanism by ridding the cell of protein aggregates and damaged organelles (6). Mitophagy is a selective form of autophagy that is specific for removal of damaged mitochondria, and mitophagy has been shown *in vitro* to be mediated by the E3 ubiquitin ligase Parkin. Parkin is recruited to damaged mitochondria by phosphatase and tensin homolog-induced putative kinase 1 (Pink1) to initi-

* This work was supported, in whole or in part, by National Institutes of Health Grants R01 DK102142, NCRR Grant 5P20RR021940, NIGMS Grants 8P20 GM103549 and T32 ES007079, NIGMS Grant Institutional Development Award P20 GM103418 (to the W.-X. D. laboratory), and Grant R01 AA020518 from the National Institute on Alcohol Abuse and Alcoholism.
[1] To whom correspondence should be addressed: Dept. of Pharmacology, Toxicology and Therapeutics, University of Kansas Medical Center, MS 1018, 3901 Rainbow Blvd., Kansas City, KS 66160. Tel.: 913-588-9813; Fax: 913-588-7501; E-mail: wxding@kumc.edu.

[2] The abbreviations used are: APAP, acetaminophen; Ad, adenovirus; ALT, alanine aminotransferase; Bort, Bortezomib; Cyp, cytochrome P450; CQ, chloroquine; HM, heavy membrane; NAPQI, *N*-acetyl-*p*-benzoquinone imine; PCNA, proliferative cell nuclear antigen; Neg, negative; 3-MA, 3-methyladenine.

ate their removal by mitophagy by performing Lys-48 and Lys-63 ubiquitination of mitochondrial outer membrane proteins (7–12).

Parkin-induced mitophagy is mainly known for its protective role in the brain because loss of Parkin has been linked to autosomal recessive parkinsonism (13). We recently found that Parkin is also ubiquitously expressed in several tissues in the mouse, including the liver (14). Therefore, we investigated the role of Parkin in mitophagy induction as a mechanism of protection in APAP-induced liver injury. We found that Parkin-induced mitophagy is likely a mechanism of protection in APAP-induced liver injury because Parkin translocated to mitochondria and increased the level of mitochondrial protein ubiquitination after APAP treatment. However, we surprisingly found that Parkin knock-out (KO) mice also had mitophagy in their livers after APAP treatment likely due to other compensatory mechanisms. In addition, Parkin KO mice were protected against APAP-induced liver injury compared with wild type (WT) mice. Mechanistically, we found that Parkin KO mice had decreased activation of c-Jun N-terminal kinase (JNK), increased induction of myeloid leukemia cell differentiation protein (Mcl-1) expression, and increased proliferation, which are all known important factors in mediating APAP-induced necrosis and liver injury. In contrast to chronic deletion of Parkin, acute knockdown of Parkin in mouse livers resulted in reduced mitophagy and Mcl-1 expression but increased JNK activation after APAP administration, which exacerbated APAP-induced liver injury. Our results thus revealed that chronic deletion (KO) and acute knockdown of Parkin differentially regulate APAP-induced mitophagy and liver injury in mice.

EXPERIMENTAL PROCEDURES

Materials—APAP was purchased from Sigma (A7085), and the kit for alanine aminotransferase (ALT) measurement was purchased from Pointe Scientific (A7526-450). The following antibodies were used for Western blot analysis: anti-Parkin (Santa Cruz Biotechnology, SC-32282); anti-ubiquitin (Santa Cruz Biotechnology, SC-8017); anti-β-actin (Sigma, A5441); anti-Cyp2e1 (Abcam, ab19140); anti-cyclin D1 (Lab Vision, RB-9041); anti-phosphorylated JNK (Cell Signaling, 4668S); anti-phosphorylated GSK-3β (Ser-9) (Cell Signaling, 5558); anti-GSK-3α/β (Cell Signaling, 5696); anti-phosphorylated glycogen synthase (Cell Signaling, 4858);, anti-JNK (BD Biosciences, 554285); anti-CoxIV (Mitosciences, MS407); anti-Mcl-1 (Rockland, 600-401-394); anti-Tom20 (Santa Cruz Biotechnology, SC11415); anti-cyclophilin D (Mitosciences, E0667); and anti-GAPDH (Cell Signaling, 2118). The APAP-adduct antibody was a gift from Dr. Lance Pohl (National Institutes of Health) (15). Anti-PCNA antibody (Santa Cruz Biotechnology, SC-56) was used for immunostaining. Horseradish peroxidase or biotin-conjugated antibodies were from Jackson ImmunoResearch. Adenovirus (Ad)-negative shRNA and Ad shRNA for mouse Parkin were purchased from Vector Biolabs (Malvern, PA).

Animal Experiments—WT C57BL/6J and whole body Parkin KO mice (C57BL/6J background, catalog no. 006582) were purchased from The Jackson Laboratory. All animals received humane treatment, and all protocols were approved by the Institutional Animal Care and Use Committee at the University of Kansas Medical Center. Eight- to 12-week-old male mice were treated with either 500 mg/kg APAP or saline by i.p. injection and were sacrificed 0.5, 1, 2, 6, or 24 h after treatment. To achieve knockdown of Parkin in mouse livers, 2-month-old male C57BL/6J mice were injected intravenously via tail vein with Ad-negative (Neg) shRNA or Ad-Parkin shRNA (1×10^9 PFU per mouse) for 4 days. Then the mice were further treated with either APAP (500 mg/kg) or saline by i.p. injection for 6 h. Liver injury was determined by measuring serum ALT. Formalin-fixed liver sections were embedded in paraffin and cut into 5-μm sections before staining with hematoxylin and eosin (H&E) to determine liver cellular necrosis.

Western Blot Analysis—Total liver lysates were prepared using RIPA buffer. Heavy membrane (HM) mainly enriched with mitochondria and cytosolic fractions were prepared as described previously (16). Briefly, liver tissues were homogenized in HIM buffer (200 mM mannitol, 70 mM sucrose, 5 mM Hepes, 0.5 mM EGTA (pH 7.5) containing protease inhibitors) using a Dounce homogenizer as we described previously (16). Homogenates were centrifuged at $1000 \times g$ to remove debris, and the supernatant was centrifuged at $10{,}000 \times g$ for 10 min to separate HM and cytosolic fractions. The supernatant was kept as the cytosolic fraction, and the pellet containing the HM fraction was further washed by centrifugation and resuspended in HIM buffer. Protein (20–30 μg) was separated by a SDS-12% polyacrylamide gel before transfer to a PVDF membrane. Membranes were probed using the indicated primary and secondary antibodies and developed with SuperSignal West Pico chemiluminescent substrate (Pierce).

PCNA Staining—Formalin-fixed liver sections were embedded in paraffin and cut into 5-μm, sections before staining with anti-PCNA antibody. Sections were deparaffinized in xylene and dehydrated in ethanol followed by incubation in hydrogen peroxide to quench peroxidases. Tissues were then blocked using Ultra V-Block (Thermo Scientific, TA-125-UB) for 5 min and incubated with PCNA antibody (1:100) overnight at 4 °C. Sections were further incubated with biotinylated secondary antibody for 30 min, and PCNA-positive cells were detected using ABC reagent (Vector, PK-6100) and DAB peroxidase substrate (Vector, SK-4105). Sections were counterstained with hematoxylin (Sigma, GHS132) for 30 s. Six fields at $\times$200 magnification were quantified for PCNA-positive cells per tissue, and results were expressed as percent PCNA-positive hepatocytes.

Primary Hepatocytes Culture—As described previously (3), murine hepatocytes were isolated from WT and Parkin KO mice by a retrograde, non-recirculating perfusion of livers with 0.05% collagenase type IV (Sigma). Cells were cultured in William's medium E with 10% fetal bovine serum but no other supplements for 2 h for attachment. Cells were then cultured in the same medium without serum overnight before treatment. All cells were maintained in a 37 °C incubator with 5% CO_2. For assessing mitochondrial membrane potential, hepatocytes were first loaded with tetramethylrhodamine methyl ester (50 nM) for 15 min and then treated with APAP (0, 5, and 10 mM) for 8 h. Cells were further stained with Hoechst 33342 (1 μg/ml) for

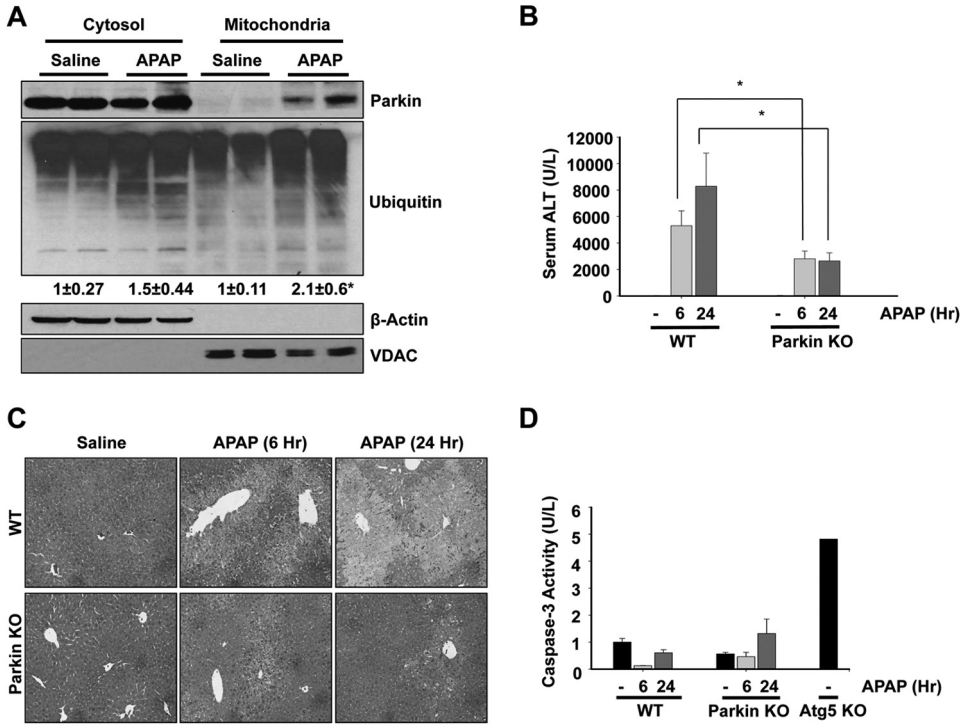

FIGURE 1. **Parkin KO mice were resistant to APAP-induced liver injury.** *A,* WT mice were treated with 500 mg/kg APAP or saline control for 6 h, and liver cytosolic and mitochondrial fractions were isolated and analyzed by Western blot. Data from two representative mice are shown. *β*-Actin and voltage-dependent anion channel (*VDAC*) were used as loading controls for cytosolic and mitochondrial fractions, respectively. Densitometry quantification of Western blots for ubiquitin is shown. Data shown are means ± S.E. ($n = 5$ for each group). Results were normalized to Actin. *, $p < 0.05$. *B,* WT and Parkin KO mice were treated with 500 mg/kg APAP or saline control for 6 or 24 h, and blood samples were measured for serum ALT. Data shown are means ± S.E. ($n \geq 5$; *, $p < 0.05$). *C,* representative H&E images are shown from WT and Parkin KO mice treated with 500 mg/kg APAP or saline control for 6 or 24 h (×100 magnification). *D,* WT and Parkin KO mice were treated with 500 mg/kg APAP or saline control for 6 and 24 h, and caspase-3 activity was measured using liver lysate. Liver lysate from a saline-treated Atg5 KO mouse was used as a positive control. Data shown are means ± S.E. ($n = 3$, no significant differences between groups).

5 min followed by fluorescence microscopy. For assessing necrosis, after APAP treatment, hepatocytes were stained with propidium iodide (1 μg/ml) for 5 min followed by fluorescence microscopy.

Caspase-3 Activity—Caspase-3 activity was determined using acetyl-DEVD-7-amino-4-trifluoromethylcoumarin fluorescent substrate (Enzo) and 20 μg of protein from mouse liver lysates after treatment with saline or APAP as we described previously (16). Liver lysate from an Atg5 KO mouse was used as a positive control (17).

GSH Measurement—GSH and glutathione disulfide (GSSG) levels in liver tissue were measured using a modified Tietze assay (18). For GSH measurement, liver tissues were homogenized in sulfosalicylic acid (3%) followed by centrifugation and dilution in potassium phosphate buffer. Samples were then subjected to a cycling reaction using glutathione reductase and dithionitrobenzoic acid, and GSH levels were determined by spectrophotometry. For GSSG, reduced GSH was removed using *N*-ethylmaleimide, and the GSSG measurement was performed using a similar spectrophotometry method as for GSH.

Analysis of Proteasome Activity—Proteasome activity was determined using a succinyl-LLVY-7-amino-4-methylcoumarin substrate (Enzo) for 20 S proteasome and 20 μg of protein from mouse liver lysates after treatment with saline or APAP as we described previously (19).

Electron Microscopy—Tissues were fixed with 2% glutaraldehyde in 0.1 M phosphate buffer (pH 7.4) followed by 1% OsO_4. After dehydration, thin sections were stained with uranyl acetate and lead citrate for observation under a JEM 1016CX electron microscope.

Statistical Analysis—Statistical analysis was conducted with Student's *t* test or one-way analysis of variance where appropriate. A $p < 0.05$ was considered significant.

RESULTS

Parkin Translocated to Mitochondria after APAP Treatment but Parkin KO Mice Were Resistant to APAP-induced Liver Injury—During Parkin-mediated mitophagy in cultured cells, it is known that Parkin translocates from the cytosol to depolarized mitochondria, resulting in mitochondrial degradation (12, 20, 21). We previously showed that APAP administration induces mitophagy in mouse livers (3). Therefore, we investigated the role of Parkin in mitophagy induction in the liver after APAP treatment. We first treated WT mice with APAP (500 mg/kg) for 6 h and determined Parkin translocation to mitochondria by Western blot analysis using cytosolic and mitochondrial fractions. Parkin translocated to mitochondria after APAP treatment, which was accompanied by increased ubiquitination of mitochondrial proteins, suggesting that Parkin may play a role in APAP-induced mitophagy (Fig. 1*A*).

To determine whether Parkin-induced mitophagy was a protective mechanism against APAP-induced liver injury, we treated WT and Parkin KO mice with APAP (500 mg/kg) for 6 and 24 h. We expected Parkin KO mice to have increased liver

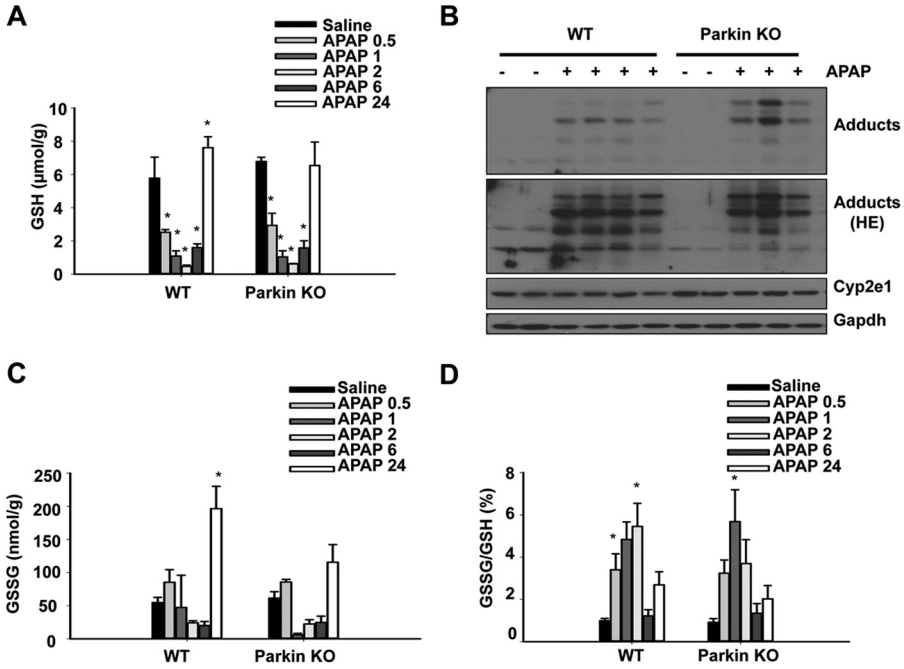

FIGURE 2. **Protection in Parkin KO mice was not due to differences in APAP metabolism or oxidative stress.** *A,* WT and Parkin KO mice were treated with 500 mg/kg APAP or saline control for 0.5, 1, 2, 6, or 24 h before measurement of liver GSH. Data shown are means ± S.E. ($n \geq 3$; *, $p < 0.05$ compared with individual saline controls, no significant differences between WT and Parkin KO mice). *B,* WT and Parkin KO mice were treated with 500 mg/kg APAP for 6 h, and total liver lysates from individual mice were analyzed by Western blot. Gapdh was used as a loading control (*HE* = high exposure). *C,* WT and Parkin KO mice were treated as in *A*, and liver GSSG was measured. Data shown are means ± S.E. ($n \geq 3$; *, $p < 0.05$ compared with WT saline control, no significant differences between WT and Parkin KO mice). *D,* ratio from results for GSH in *A* and GSSG in *C* are further calculated. Data shown are means ± S.E. (*, $p < 0.05$ compared with individual saline controls, no significant differences between WT and Parkin KO mice).

injury after APAP treatment due to an inability to induce mitophagy. However, we surprisingly found that Parkin KO mice were protected from APAP-induced liver injury compared with WT mice (Fig. 1, *B* and *C*). Parkin KO mice had significantly less liver injury compared with WT mice after APAP treatment for 6 and 24 h as determined by serum ALT levels. WT mice had a mean serum ALT of 5309 units/liter at 6 h and 8290 units/liter at 24 h, and KO mice had a mean serum ALT of 2813 units/liter at 6 h and 2649 units/liter at 24 h (Fig. 1*B*). WT mice also had a significantly greater area of hepatocellular necrosis than KO mice after APAP treatment for 6 and 24 h as determined by H&E staining. Saline-treated WT and Parkin KO mice did not develop any cellular necrosis (Fig. 1*C*).

APAP is well known to induce cell death via necrosis and not apoptosis (22), so we ensured that protection in Parkin KO mice was not due to APAP induction of cell death via apoptosis instead of necrosis by assessing caspase-3 activity in liver tissue lysates. Neither WT nor Parkin KO mice had any induction of caspase-3 activity after APAP treatment, indicating that APAP did not induce apoptosis in WT or Parkin KO mice, as expected. Lysate from an Atg5 KO mouse was used as a positive control for caspase-3 activation (Fig. 1*D*).

Protection in Parkin KO Mice Was Not Due to Differences in APAP Metabolism or Oxidative Stress—APAP is metabolized primarily by Cyp2e1 to its reactive metabolite NAPQI, which is detoxified by GSH at therapeutic doses. GSH is depleted during APAP overdose, which allows for NAPQI to form protein adducts and induce mitochondrial damage and subsequent hepatocellular necrosis (22).To ensure that protection in KO mice was not due to differences in APAP metabolism, we treated WT and Parkin KO mice with APAP (500 mg/kg) or saline control and measured GSH levels 0.5, 1, 2, 6, and 24 h after treatment. WT and Parkin KO mice had similar basal levels of GSH and similar GSH depletion at 0.5, 1, and 2 h after APAP treatment. WT and Parkin KO mice also had similar recovery of GSH after APAP treatment for 6 and 24 h (Fig. 2*A*). Furthermore, WT and Parkin KO mice had similar levels of protein adducts and Cyp2e1 protein expression after APAP or saline treatment for 6 h (Fig. 2*B*). These results suggest that protection in Parkin KO mice was not due to differences in metabolism of APAP between WT and Parkin KO mice.

GSSG levels and the ratio of GSSG to GSH are markers of oxidative stress. WT and Parkin KO mice had similar basal GSSG levels and GSSG to GSH ratio. WT and Parkin KO mice also had similar GSSG levels and GSSG to GSH ratios after APAP treatment for 0.5, 1, 2, and 6 h. Parkin KO mice had slightly less GSSG than WT mice after APAP treatment for 24 h, but the decrease in KO mice was not significant compared with WT mice (Fig. 2, *C* and *D*). These results suggest that differences in injury between WT and Parkin KO mice were not due to differences in oxidative stress.

Mitophagy Occurred in Both WT and Parkin KO Mice after APAP Treatment—We compared and quantified the number of autophagosomes and lysosomes containing mitochondria (hereafter referred to as mitophagosomes) by electron microscopy (EM) between WT and Parkin KO mice after APAP treatment. We also performed an autophagy flux assay with a combination of APAP and chloroquine (CQ) treatment. CQ blocks lysosome degradation, which allows for accurate quantification of autophagosome and lysosome components (23). Treatment

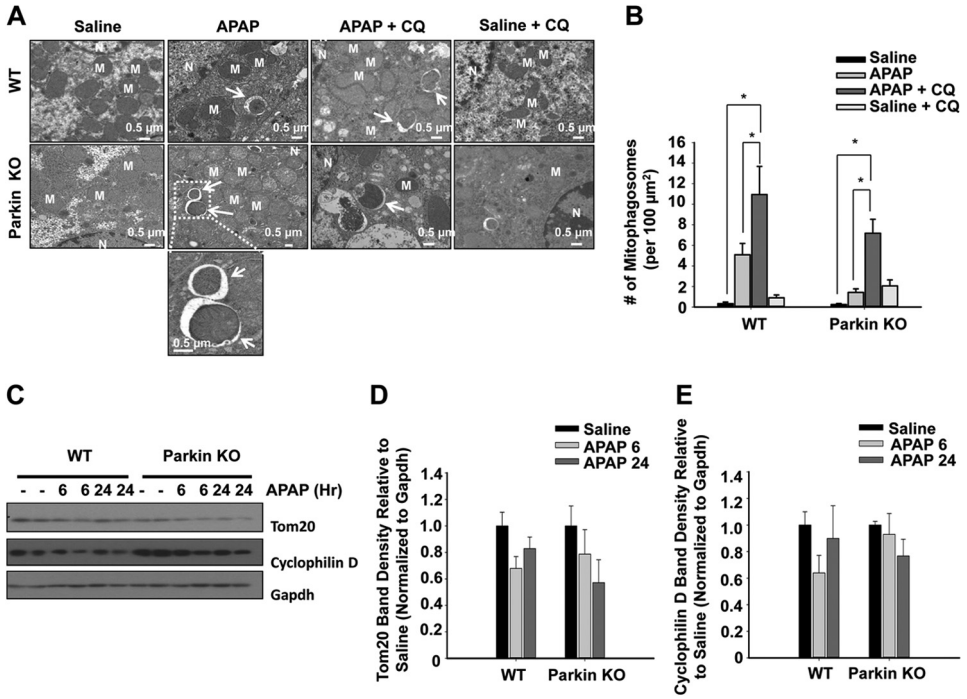

FIGURE 3. **Mitophagy occurred in both WT and Parkin KO mice after APAP treatment.** *A,* representative EM images are shown from WT and Parkin KO mice treated with APAP (500 mg/kg) with or without CQ (60 mg/kg) for 6 h. An enlarged image of mitophagosomes is shown from the *dotted line boxed* area (*arrows,* mitophagosomes; *M,* mitochondria; *N,* nucleus). *B,* quantification of EM images. Data shown are means ± S.E. ($n \geq 2$ mice per group, at least 10 images quantified per group; *, $p < 0.05$, no significant differences between WT and Parkin KO mice). *C,* WT and Parkin KO mice were treated with 500 mg/kg APAP or saline control for 6 and 24 h, and total liver lysates were analyzed for mitochondrial protein degradation by Western blot. Gapdh was used as a loading control. Results for two individual mice are shown. *D* and *E,* densitometry quantification of Western blots for Tom20 and cyclophilin D. Data shown are means ± S.E. ($n = 4$ for each group, no significant differences among groups). Results were normalized to Gapdh.

with APAP significantly increased the number of mitophagosomes, which was further enhanced in the presence of CQ in WT mice, indicating that APAP induces mitophagy flux in mouse livers. Surprisingly, Parkin KO mice also had an increased number of mitophagosomes, which was also further enhanced by the presence of CQ treatment, although the number of mitophagosomes was lower compared with WT mice (Fig. 3, *A* and *B*).

WT and Parkin KO mice also showed slight degradation of the mitochondrial outer membrane protein Tom20 as well as the mitochondrial matrix protein cyclophilin D after APAP treatment (Fig. 3, *C–E*). We recently reported that APAP treatment in mice causes distinctive mitochondrial changes within different zones of the mouse liver. In addition to mitophagy, APAP also induces mitochondrial biogenesis adjacent to the necrotic areas likely to promote liver repair (4). This could offset the levels of mitochondrial degradation mediated by mitophagy using the total liver lysates. A better quantitative approach, such as the use of micro-dissection to isolate tissues from different zones of the liver, may need to be established in the future. Taken together, these results indicate that APAP may induce mitophagy in mouse livers through Parkin-dependent and -independent mechanisms.

Parkin KO Mice Had Decreased JNK Activation and Increased Mcl-1 Expression Compared with WT Mice after APAP Treatment—Activation of JNK by phosphorylation and its translocation to the mitochondria are well known to exacerbate APAP-induced liver injury (24–27). To determine whether WT and Parkin KO mice had differences in JNK activation, we measured protein levels of phosphorylated JNK (pJNK) in WT and Parkin KO mouse livers after APAP treatment for 2 and 6 h. Parkin KO mice had slightly less JNK activation 2 h after APAP treatment compared with WT mice, and JNK activation was significantly less in Parkin KO mice compared with WT mice 6 h after APAP treatment (Fig. 4, *A* and *B*). WT and Parkin KO mice had similar levels of total JNK protein expression (Fig. 4*A*). In addition, we investigated mitochondrial JNK activation using cytosolic and mitochondrial fractions from WT and Parkin KO mouse liver lysates after APAP treatment for 6 h. We found that JNK translocated to mitochondria after APAP treatment, and the level of total JNK levels on mitochondria was surprisingly higher in Parkin KO mice compared with WT mice (Fig. 4, *C* and *D*). However, the active form of JNK (pJNK) on mitochondria was much lower in Parkin KO mice compared with WT mice after APAP treatment (Fig. 4, *C* and *D*). There results suggest that Parkin may promote JNK activation once it is translocated to mitochondria, and the regulation of mitochondrial JNK translocation is independent of Parkin.

Mcl-1 is an anti-apoptotic protein that has been shown to be protective against APAP-induced liver injury (28, 29). We measured protein levels of Mcl-1 using total lysate from WT and Parkin KO mouse livers 6 h after APAP treatment. Mcl-1 protein expression was increased after APAP treatment in both WT and Parkin KO mice, and Parkin KO mice had higher basal levels of Mcl-1, which were sustained after APAP treatment compared with WT mice (Fig. 5, *A* and *B*). It has been reported that GSK-3β phosphorylates Mcl-1 and promotes its protea-

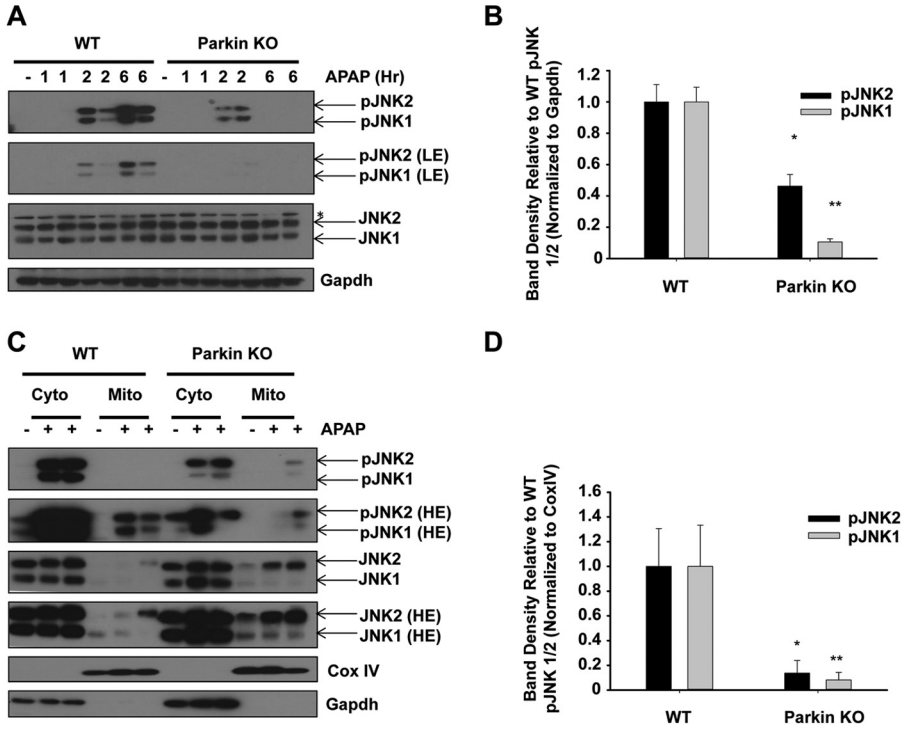

FIGURE 4. **Protection in Parkin KO mice may be due to decreased JNK activation.** *A,* WT and Parkin KO mice were treated with 500 mg/kg APAP or saline control for 1, 2, or 6 h, and total liver lysates were analyzed by Western blot. Results from one representative mouse are shown for saline, and results from two representative mice are shown for APAP treatment. Gapdh was used as a loading control (*LE,* low exposure). *B,* densitometry quantification of pJNK. Data shown are means ± S.E. ($n = 2$ each for WT and Parkin KO saline, 3 each for WT and Parkin KO APAP-treated mice; *, $p < 0.05$ compared with WT APAP treatment at 6 h; **, $p < 0.05$ compared with WT APAP treatment at 24 h). Results were normalized to Gapdh. *C,* WT and Parkin KO mice were treated with 500 mg/kg APAP or saline control for 6 h, and cytosolic and mitochondrial fractions were analyzed by Western blot. CoxIV and Gapdh were used as loading controls for HM and cytosolic fractions, respectively (*HE,* high exposure). *D,* densitometry quantification of pJNK in the mitochondrial fraction. Data shown are means ± S.E. ($n = 2$ each for WT and Parkin KO saline treated mice, 3 each for WT and Parkin KO APAP-treated mice; *, $p < 0.05$ compared with WT APAP treatment at 6 h; **, $p < 0.05$ compared with WT APAP treatment at 24 h). Results were normalized to CoxIV.

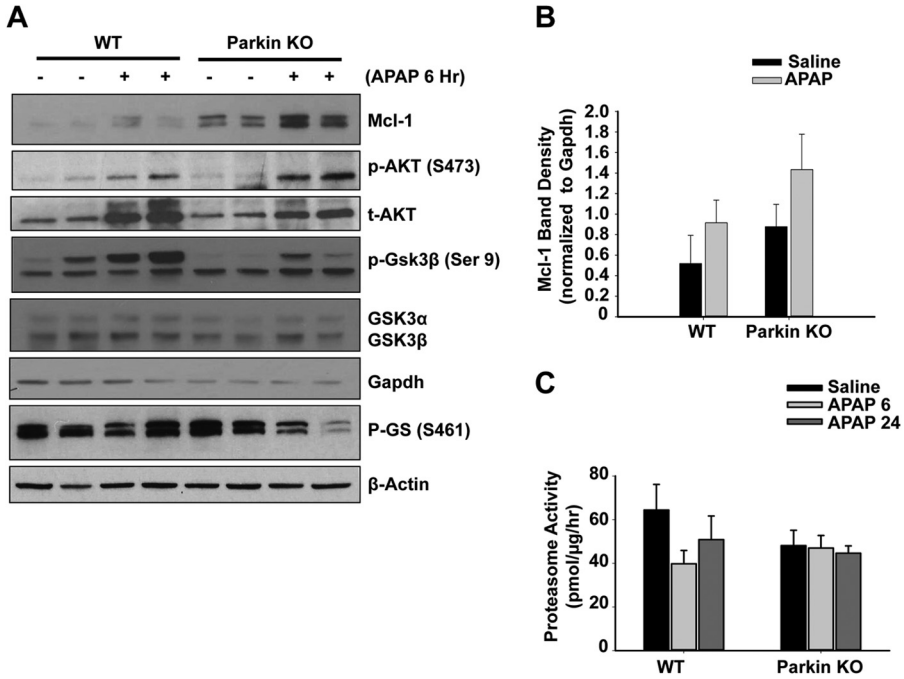

FIGURE 5. **Parkin KO mice had increased levels of Mcl-1 proteins after APAP treatment.** *A,* WT and Parkin KO mice were treated with 500 mg/kg APAP or saline control for 6 h, and total liver lysates were analyzed by Western blot. Gadph was used as a loading control. *B,* densitometry quantification of Western blots for Mcl-1. Data shown are means ± S.E. ($n = 4$ per group). Results were normalized to Gapdh. *C,* WT and Parkin KO mice were treated with 500 mg/kg APAP or saline control for 6 and 24 h. Twenty micrograms of total liver lysates were used to measure the 20 S proteasomal activity using a fluorogenic substrate. Results are presented as means ± S.E. from four different mice.

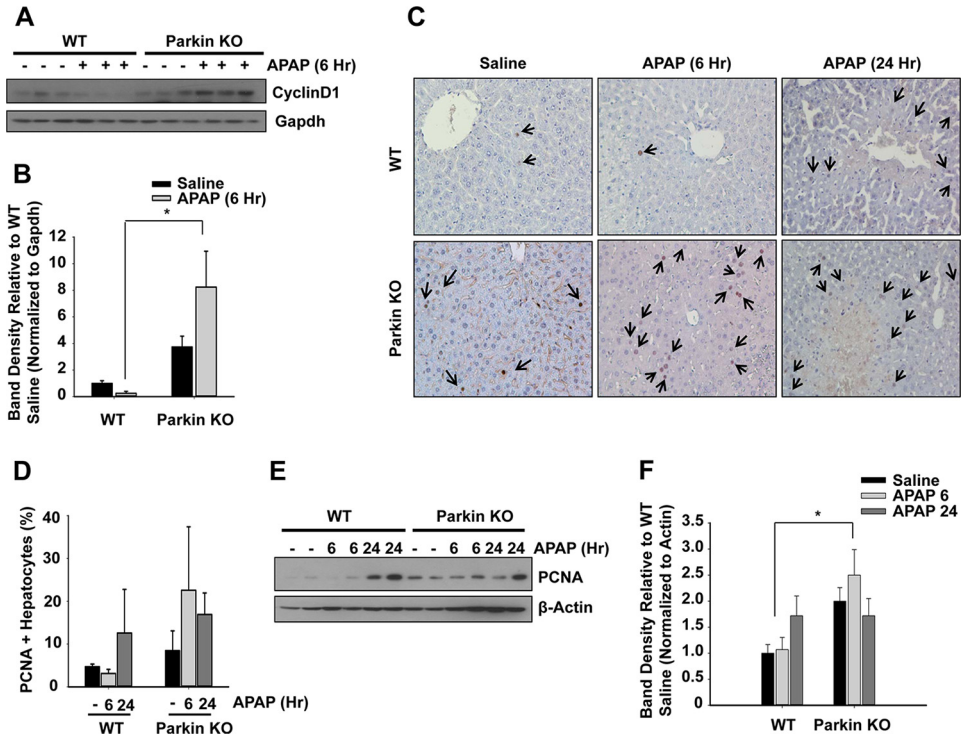

FIGURE 6. **Protection in Parkin KO mice may be due to increased hepatocyte proliferation.** *A,* WT and Parkin KO mice were treated with 500 mg/kg APAP or saline control for 6 h, and total liver lysates were analyzed by Western blot. *B,* densitometry quantification of Western blots for cyclin D1. Data shown are means ± S.E. ($n = 4$ per group). Results were normalized to Gapdh. *C,* representative images from PCNA staining are shown (*arrows* represent PCNA-positive hepatocytes). *D,* PCNA staining quantification. Results are presented as % PCNA-positive hepatocytes. Data shown are means ± S.E. ($n = 3$, ×100 magnification, no significant differences between groups). Six images were quantified per liver tissue. *E,* mice were treated as in *A,* and total liver lysates were analyzed by Western blot. *F,* densitometry quantification of Western blots for PCNA. Data shown are means ± S.E. ($n = 3$–4 per group; *, $p < 0.05$). Results were normalized to β-actin.

somal degradation (30). We found that APAP treatment increased the phosphorylation levels of Akt and GSK-3β at serine 9 in both WT and Parkin KO mouse livers. Because Akt-mediated Ser-9 phosphorylation of GSK-3β negatively regulates its activity, we also determined the phosphorylated levels of glycogen synthase, which is one of the substrates of GSK-3β. We found that there was a dramatic reduction in phosphorylated levels of glycogen synthase in Parkin KO but not WT mouse livers after APAP treatment (Fig. 5*A*), suggesting decreased GSK-3β activity in APAP-treated Parkin KO mouse livers.

It is known that Mcl-1 is degraded by the ubiquitin proteasome system (30, 31), and APAP treatment tended to slightly decrease proteasome activity in WT mice, but these changes did not reach statistical differences (Fig. 5*C*). In addition, Parkin KO mice overall tended to have slightly decreased proteasome activity, although APAP treatment did not further alter the proteasome activity, and these changes were also not statistically different (Fig. 5*C*). Collectively, these data suggest that protection in Parkin KO mice against APAP-induced liver injury was likely due to decreased JNK activation and increased Mcl-1 expression.

Parkin KO Mice Had Increased Proliferation Compared with WT Mice—Following APAP-induced cellular necrosis, it is well known that the liver has the capacity for repair and complete recovery if the level of injury is not too severe. Parkin KO mice have previously been shown to have increased proliferation leading to the eventual development of hepatocellular carcinoma at 18 months (32, 33). Therefore, we evaluated proliferation levels in WT and Parkin KO mice after APAP treatment to determine whether greater levels of hepatocyte proliferation could be an additional mechanism of protection against APAP-induced liver injury in KO mice. Parkin KO mice had significantly increased basal expression levels of the proliferation proteins cyclin D1 and PCNA compared with WT mice. In addition, Parkin KO mice had increased expression of these proliferative proteins compared with WT mice after APAP treatment for 6 h as shown by cyclin D1 and PCNA Western blot analysis (Fig. 6, *A, B, E,* and *F*). Immunohistochemistry for PCNA staining also revealed an increase for the number of PCNA-positive cells in APAP-treated Parkin KO mice compared with APAP-treated WT mice, but these changes did not reach statistical significance (Fig. 6, *C–D*). This was likely due to large variations in the immunohistochemistry analysis from the limited liver areas that we could assess in each sample, although we have counted six random images from each sample. Nevertheless, these data suggest that increased proliferation levels in Parkin KO mice may provide protection against APAP-induced liver injury by allowing for faster replacement of necrotic hepatocytes and subsequent regeneration compared with WT mice.

APAP Treatment Induced Proteasomal Degradation of Mcl-1 and Necrosis in Cultured Mouse Hepatocytes Independent of Parkin—To further determine whether the proteasome plays a role in APAP-induced changes of Mcl-1, we treated primary cultured mouse hepatocytes with APAP in the presence or

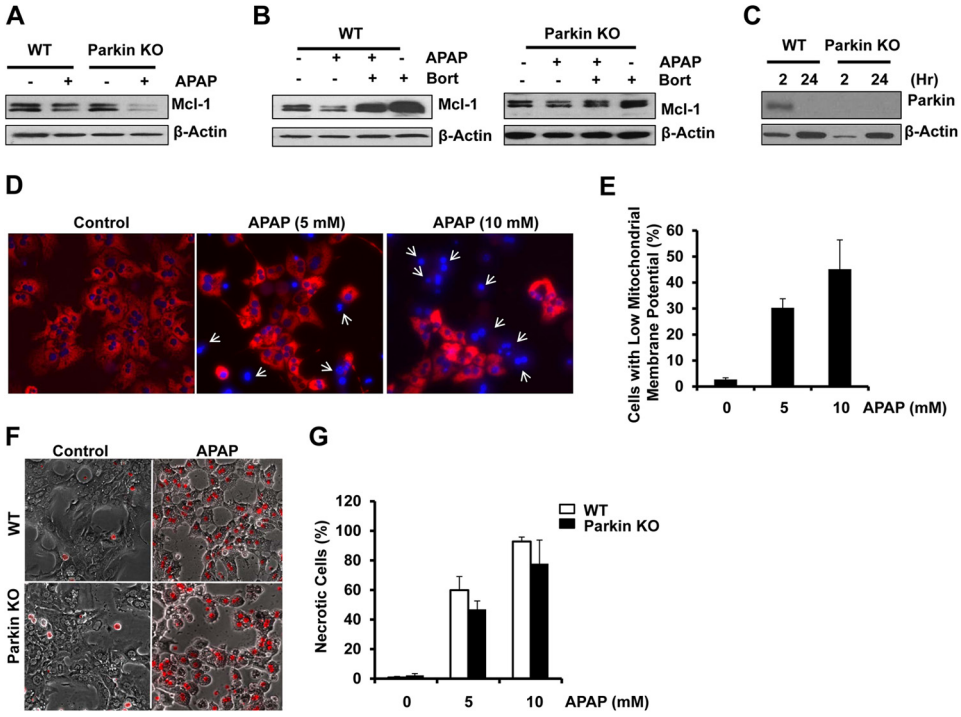

FIGURE 7. **APAP-induced Mcl-1 degradation and necrosis in cultured mouse hepatocytes independent of Parkin.** *A* and *B*, isolated hepatocytes from WT and Parkin KO mice were treated with APAP (10 mM) for 6 h in the presence or absence of Bort (50 nM). Total cell lysates were subjected to Western blot analysis. *C*, isolated hepatocytes from WT and Parkin KO mice were cultured for 2 and 24 h. Total cell lysates were subjected to Western blot analysis for Parkin. Representative blots from three independent experiments are shown. *D*, hepatocytes were first loaded with tetramethylrhodamine methyl ester (50 nM) for 15 min and then treated with APAP for 8 h. Cells were further stained with Hoechst 33342 (1 μg/ml) for 5 min followed by fluorescence microscopy. The representative overlaid images are shown. *Arrows* denote the cells with loss of mitochondrial membrane potential. *E*, number of cells with loss of mitochondrial membrane potential was quantified. Data are means ± S.E. from three independent experiments (More than 300 hundred cells were counted in each experiment from 3 to 4 different fields; *, $p < 0.05$.) *F*, WT and Parkin KO hepatocytes were treated with APAP for 24 h, and cells were stained with propidium iodide (1 μg/ml) for 5 min followed by microscopy. Representative phase-contrast images overlaid with propidium iodide signals are shown. *G*, percentage of PI-positive cells was quantified. Data shown are means ± S.E. from three independent experiments (at least three different images were randomly chosen from each experiment and more than 300 cells were counted; *n.s.*, statistically no significance).

absence of Bortezomib (Bort), a proteasome inhibitor. Unlike the *in vivo* mouse liver, there was no difference in basal levels of Mcl-1 between the hepatocytes isolated from WT and Parkin KO mice. APAP treatment decreased Mcl-1 levels, which were recovered by Bort in both WT and Parkin KO hepatocytes. Treatment with Bort also increased Mcl-1 levels compared with control hepatocytes regardless of Parkin (Fig. 7, *A* and *B*). These results indicate that APAP-induced changes of Mcl-1 are mediated by the proteasome. Intriguingly, WT hepatocytes lost the expression of Parkin after 24 h of culture (Fig. 7*C*), which is a time point that we had started to treat hepatocytes with drugs including APAP in our previous studies (3, 34). We found that APAP treatment for 8 h increased the number of cells with decreased mitochondrial membrane potential (Fig. 7, *D* and *E*). Most cells lost mitochondrial membrane potential after APAP treatment for 24 h (data not shown). Consistent with our previous findings, APAP treatment also increased necrotic cells in WT hepatocytes. Interestingly, we found that there was no difference in APAP-induced necrosis between WT and Parkin KO hepatocytes (Fig. 7, *F* and *G*). Taken together, Parkin is dispensable for APAP-induced Mcl-1 degradation and necrosis in primary cultured mouse hepatocytes.

Acute Knockdown of Parkin in Mouse Livers Impaired Mitophagy and Exacerbated APAP-induced Liver Injury—Because Parkin KO mice have no obvious phenotypes, it is possible that the mice may develop compensatory and adaptive mechanisms for the chronic loss of Parkin, which may contribute to the resistance to APAP-induced liver injury that we found in this study. To overcome the potential compensation and adaptation by the chronic loss of Parkin, we determined APAP-induced mitophagy and liver injury after acute knockdown of Parkin in mouse livers using an Ad-shRNA approach. We found that Ad-Parkin shRNA by tail vein injection dramatically reduced the expression of Parkin in mouse livers but had no effect on the expression of Parkin in mouse pancreas or skeletal muscle (Fig. 8*A*). In contrast to Parkin KO mice, mice given Ad-Parkin shRNA had increased serum ALT levels and hepatic necrosis compared with mice given Ad-Neg shRNA (Fig. 8, *B* and *C*). Notably, mice that received adenovirus treatment had decreased sensitivity to APAP administration because ALT levels were less compared with the nonvirus-infected mice that were treated with the same dose of APAP (Fig. 1*B*). Our results are consistent with a previous study that showed reduced susceptibility to APAP after viral infection in mice (35). There were no significant differences in Cyp2e1 or APAP adducts levels between Ad-Parkin and Ad-Neg shRNA-treated groups, but Ad-Parkin shRNA markedly decreased hepatic Parkin expression (Fig. 8*D*).

The Ad-Parkin shRNA-treated mice had increased phosphorylated levels of JNK but decreased levels of Mcl-1 and PCNA compared with Ad-Neg shRNA-treated mice after

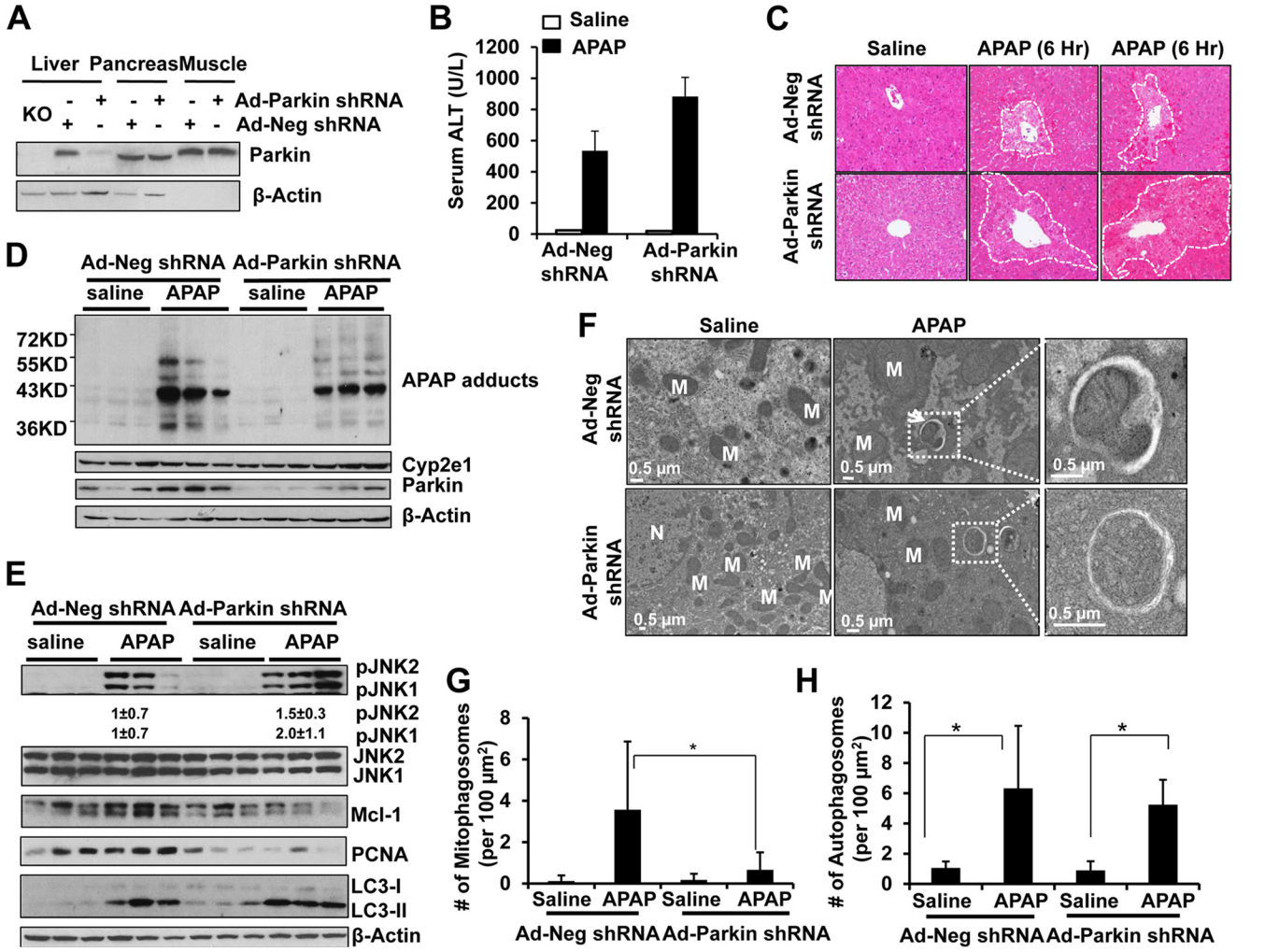

FIGURE 8. **Acute knockdown of Parkin in mouse livers impaired with APAP-induced mitophagy and exacerbated APAP-induced liver injury.** *A,* male C57Bl/6J mice were treated either with Ad-Neg or Ad-Parkin shRNA (i.v., 1×10^9 pfu per mouse) for 4 days. Total liver, pancreas, and skeletal muscle lysates were subjected to Western blot analysis. Lysate from a Parkin KO mouse liver was used a negative control. Mice were further treated with APAP (500 mg/kg) or saline for another 6 h. *B,* blood samples were used to measure serum ALT levels. Data shown are means ± S.E. ($n = 4$; *, $p < 0.05$). *C,* representative H&E images are shown (×200 magnification). *Dotted line circled areas* denote centrilobular necrosis. *D* and *E,* total liver lysates were subjected to Western blot analysis. Densitometry quantification of Western blots for p-JNK1 and p-JNK2 ($n = 3$ per group). Results were normalized to *β*-actin. *F,* representative EM images are shown. An enlarged image of a mitophagosome showing an enveloped mitochondrion and an enlarged image of an autophagosome showing enveloped cytosolic proteins are from the *dotted line boxed areas* (*arrow* = mitophagosomes, *M* = mitochondria, and *N* = nucleus). *G* and *H,* quantification of EM images for mitophagosomes and total autophagosomes. Data shown are means ± S.E. ($n \geq 20$ images quantified per group; *, $p < 0.05$).

administration of APAP (Fig. 8*E*). The levels of LC3-II, a marker for autophagy, were increased after APAP treatment in both Ad-Neg and Ad-Parkin-treated mice (Fig. 8*E*), suggesting that APAP increased the numbers of autophagosomes/autolysosomes independent of Parkin. Moreover, the number of mitophagosomes was significantly decreased in mouse livers treated with Ad-Parkin shRNA compared with Ad-Neg shRNA after administration of APAP (Fig. 8, *F* and *G*). Consistent with the LC3-II results from Western blot analysis, the number of total autophagosomes was very comparable between groups of Ad-Parkin shRNA and Ad-Neg shRNA after administration of APAP (Fig. 8*H*), suggesting that acute knockdown of Parkin does not affect the general autophagy. These results suggest that acute knockdown of Parkin in mouse livers had impaired mitophagy and hepatocyte proliferation, decreased hepatic Mcl-1 expression, and increased JNK activation, which exacerbated liver injury in response to APAP administration.

DISCUSSION

In this study, we found that APAP treatment induced Parkin translocation to mitochondria and increased levels of mitochondrial protein ubiquitination in WT mouse livers. However, we found that Parkin differentially regulated mitophagy and APAP-induced liver injury depending on whether Parkin was chronically deleted in mice or acutely knocked down in mouse livers. We found that mitophagy still occurred in Parkin KO mouse livers after APAP treatment, suggesting that Parkin may be dispensable for mitophagy under chronic Parkin loss conditions. Moreover, we surprisingly found that Parkin KO mice were protected against APAP-induced liver injury compared with WT mice. In contrast, mice with acute knockdown of Par-

kin had decreased hepatic mitophagy and increased APAP-induced liver injury.

Parkin Was Dispensable for APAP-induced Mitophagy in Parkin KO Mice but Not in Mice with Acute Knockdown of Hepatic Parkin—Parkin translocated to mitochondria after APAP treatment in WT mice, which correlated with an increase in mitochondrial protein ubiquitination, suggesting that Parkin-induced mitophagy occurs in mouse liver after APAP treatment. However, we found Parkin KO mice had similar mitochondrial protein degradation after APAP treatment, although there was a slight reduction in the number of mitophagosomes in Parkin KO mice compared with WT mice. Mitophagy is likely a protective mechanism against APAP-induced liver injury by promoting removal of damaged mitochondria in both WT and Parkin KO mice. However, it appears that Parkin is not required for mitophagy induction in the liver because mitophagy still occurred in Parkin KO mouse livers after APAP treatment. In contrast, mice with acute knockdown of Parkin had significantly reduced mitophagy after APAP administration. These results suggest that alternative compensatory mechanisms for mitophagy independent of Parkin may occur when Parkin is chronically deleted in mice after APAP administration. To support this notion, it was previously reported that compensatory mitophagy also occurred in Parkin KO mouse hearts (36). It is likely that compensatory and adaptive alternative mechanisms for mitophagy independent of Parkin cannot be established within the relatively short time period after acute Parkin knockdown. Alternatively, although it seems to be less likely that the loss of Parkin in other tissues in Parkin KO mice may also affect the mitophagy signaling pathway in the liver, the tissue cross-talk regulating mitophagy in the liver is currently unknown.

It was recently reported that at least three distinct types of mitophagy could occur in hepatocytes as follows: 3-methyladenine (3-MA)-sensitive; 3-MA-insensitive, and mitochondrion-derived vesicles (37, 38). We previously showed that 3-MA inhibited APAP-induced autophagy and enhanced APAP-induced necrosis in cultured mouse hepatocytes (3). These results suggest that APAP may induce 3-MA-sensitive mitophagy. In addition to canonical mitophagy, we also showed that APAP could induce the formation of mitochondrial spheroids, a process of mitochondria remodeling that forms unique vesicle-like structures derived directly from mitochondria in mouse livers (4, 39).

The identification of mitophagy in Parkin KO mice after APAP administration suggests that Parkin may not be essential for mitophagy induction *in vivo*. The mechanism for alternative Parkin-independent mitophagy induction in the liver is currently unknown but could be due to up-regulation of other important proteins or pathways in the absence of Parkin that have been shown to have a role in the mitophagy pathway. For example, Parkin-independent mitophagy in Parkin KO mice may be mediated by another E3 ubiquitin ligase, such as March5, Smurf1, or Mulan. In addition, Parkin-independent mitophagy may occur via Bcl2/adenovirus E1B 19-kDa interacting protein 3 (Bnip3), Fun14 domain containing 1 (Fundc1), or Nix. Bnip3 and Fundc1 have both been shown to play a role in mitophagy induction for removal of damaged mitochondria to prevent accumulation of reactive oxygen species during hypoxia (40, 41). Nix also plays a role in selective removal of mitochondria during red blood cell maturation (42–44). In addition, Nix has been shown to play a role in Parkin-dependent mitophagy induction by promoting mitochondrial depolarization and translocation of Parkin to mitochondria (21). Cardiolipin, a phospholipid located on the inner mitochondrial membrane, has also been recently shown to have a role in mitophagy induction in neurons by translocating to the outer mitochondrial membrane and interacting with the autophagosome protein microtubule-associated protein light chain 3 (LC3) (45, 46). Therefore, cardiolipin may also have a role in Parkin-independent mitophagy induction in the liver. Even though the mechanism of Parkin-independent mitophagy induction in the liver is not currently understood, induction of mitophagy in both WT and Parkin KO mouse livers was likely a mechanism of protection against APAP-induced liver injury by removing damaged mitochondria. However, in addition to mitophagy, Parkin KO mice had other protective mechanisms against APAP-induced liver injury and necrosis compared with WT mice, which are further discussed below.

JNK Activation Was Differentially Regulated in Parkin KO and Acute Parkin Knockdown Mice after APAP Treatment—Another mechanism of protection in Parkin KO mice was decreased JNK activation compared with WT mice after APAP treatment. JNK activation, particularly in the mitochondria, has been shown to exacerbate APAP-induced liver injury (24, 25, 27, 47).

Parkin has been previously shown to negatively regulate JNK activity in *Drosophila* (48, 49). Parkin-mutant flies contained high levels of phosphorylated JNK in their dorsomedial neurons, resulting in shrinkage of the neuronal cell body, which was not present in control flies. Neuron cell body morphology was normal when Parkin-mutant flies were treated with a dominant negative form of JNK, confirming that the morphology changes were caused by increased JNK activation in the absence of Parkin (49). Parkin was also found to suppress JNK activation in the *Drosophila* eye during development by transcriptionally repressing *basket (bsk*), which is a gene encoding for JNK (48). In addition, Parkin was shown to suppress JNK activation *in vitro* in EPP85 human pancreatic carcinoma cells via mono-ubiquitination of heat-shock protein 70 (HSP70), but the exact mechanism for how mono-ubiquitinated HSP70 inhibits activation of JNK is unknown (50). Furthermore, Parkin was shown to inhibit JNK activity in COS1 monkey kidney fibroblasts (49). Parkin and JNK were co-transfected into COS1 cells, and co-expression of Parkin reduced JNK activation (49). Consistent with these findings, we found that APAP increased JNK activation in acute Parkin knockdown mouse livers. In contrast, JNK activation was decreased in Parkin KO mouse livers compared with WT mice after APAP treatment. These results suggest that acute knockdown and chronic loss of Parkin differentially impact JNK activation, which is likely due to induction of some adaptive mechanisms in mouse livers when Parkin is chronically absent.

The adaptive mechanisms for JNK inhibition after APAP treatment in Parkin KO mice is currently unknown but may involve mono- or polyubiquitination of upstream or down-

stream mediators of JNK activation. For example, chronic loss of Parkin may affect the degradation of MAPK phosphatase-1 (MkP-1), an endogenous inhibitor of JNK activation (51). Parkin has also been shown to stabilize proteins via monoubiquitination, so chronic loss of Parkin may also stabilize upstream activators of JNK such as apoptosis signal-regulating kinase 1 (Ask1) via monoubiquitination (52). Taken together, it appears that chronic and acute Parkin loss have contrasting impacts on JNK activation in mouse livers after APAP treatment, which may subsequently protect against or exacerbate APAP-induced liver injury.

Mcl-1 Expression Was Differentially Regulated in Parkin KO or Acute Parkin Knockdown Mice after APAP Treatment—Mcl-1 is an anti-apoptotic Bcl-2 protein that is mostly localized to the mitochondrial membrane (53), and its stabilization has been shown to play a protective role against APAP-induced hepatocellular necrosis (28). Parkin KO mice had increased liver Mcl-1 expression compared with WT mice before and after APAP treatment, which may be another mechanism for their protection against APAP-induced liver injury. APAP has been shown to induce degradation of Mcl-1 in the early phase of liver injury in starved mice (1–4 h after treatment) (29), but we did not observe degradation of Mcl-1 in WT or Parkin KO mice after APAP treatment in fed mice. We actually observed an increase in Mcl-1 expression after APAP treatment. This discrepancy could be due to several possibilities. First, in this study, we used fed mice to avoid the possible interference of starvation-induced autophagy, whereas Shinohara *et al.* (29) used starved animals. Starvation may inactivate AKT and interfere with AKT-GSK3β-mediated Mcl-1 phosphorylation and proteasomal degradation. Consistent with this notion, we also found that APAP decreased Mcl-1 in primary cultured hepatocytes in serum-free medium.

Second, we assessed APAP-induced liver injury 6 h after treatment, which may allow for recovery of Mcl-1 protein levels. Third, Mcl-1 expression is regulated by Gsk-3β phosphorylation, which primes it for ubiquitination and degradation by the proteasome (30). Gsk-3β is known to translocate to mitochondria after APAP-induced liver injury where it phosphorylates Mcl-1 to initiate its proteasomal degradation (29). Because phosphorylation of GSK-3β at serine 9 normally inhibits its activity (54), increased serine 9 phosphorylation of GSK-3β may thus contribute to the increased Mcl-1 levels following APAP treatment. Fourth, Parkin KO mice tend to have decreased proteasomal activity compared with WT mice, which may also partially contribute to increased Mcl-1 protein expression compared with WT mice. In primary cultured mouse hepatocytes, it seems that Parkin is less important in regulating Mcl-1 levels after APAP treatment because WT hepatocytes lost the expression of Parkin during culture and APAP decreased Mcl-1 protein levels in both cultured WT and Parkin KO hepatocytes. The decreased Mcl-1 protein levels were reversed by a proteasome inhibitor, supporting the important role of the proteasome in regulating Mcl-1 levels in APAP-treated hepatocytes. Finally, Mcl-1 degradation has also been shown to be induced by JNK phosphorylation in HeLa cells (55). Parkin KO mice had reduced JNK activation, which may be linked to their increased Mcl-1 expression. We found that acute knockdown of Parkin in mouse livers had decreased Mcl-1 protein levels after APAP treatment in mouse livers. Interestingly, Parkin knockdown mice also had increased JNK activation in their livers after APAP treatment, which is opposite from APAP-treated Parkin KO mouse livers. These findings are also in line with the known role of JNK in regulating Mcl-1.

In addition, the mammalian target of rapamycin pathway has also been shown to have a role in Mcl-1 transcriptional regulation in Parkin KO mouse neurons because neurons in Parkin KO mice had increased Mcl-1 expression due to compensatory activation of the mammalian target of rapamycin (56). Future work is needed to determine the exact role of JNK and the mammalian target of rapamycin in regulating Mcl-1 during APAP overdose.

It should also be noted that the previous work by Shinohara *et al.* (29) and this study only indicate an association of Mcl-1 with APAP-induced hepatotoxicity. In an attempt to determine the exact contribution of Mcl-1 on APAP-induced liver injury, we injected mice with Bort and determined the hepatic proteasome activity, Mcl-1 levels, and APAP-induced liver injury. Although we did find that Bort dramatically inhibited hepatic proteasome activities and elevated Mcl-1 levels in mouse livers, Bort treatment did not protect but rather worsened APAP-induced liver injury (data not shown). This was likely due to increased levels of APAP adducts along with other proteins that are also subjected to proteasome inhibition, which suggests that pharmacological inhibition of the proteasome is not an appropriate approach to address the specific role of Mcl-1 in APAP-induced hepatotoxicity. Future work using genetic shRNA knockdown of hepatic Mcl-1 or using liver-specific Mcl-1 knock-out mice may be a better approach to further determine the role of Mcl-1 in APAP-induced hepatotoxicity.

Increased Hepatocyte Proliferation in Parkin KO Mice but Not in Mice with Acute Knockdown of Parkin after APAP Treatment—Parkin KO mice had increased basal hepatocyte proliferation levels and increased hepatocyte proliferation after APAP treatment for 6 and 24 h, which may provide protection against APAP-induced hepatocellular necrosis and liver injury by allowing for faster replacement of necrotic hepatocytes. Parkin has been previously shown to be a tumor suppressor in liver, and Parkin KO mice develop spontaneous liver tumors around 18 months of age (32). In addition, Parkin expression is significantly decreased or absent in most cancer cell lines and human liver tumors (33). This tumor-suppressive function of Parkin was likely important in protection against APAP-induced liver injury, which causes significant hepatocellular necrosis. With increased basal proliferation and increased proliferation after APAP treatment compared with WT mice, Parkin KO mice were likely able to replace their necrotic hepatocytes faster than WT mice, making them resistant to APAP-induced hepatocellular necrosis and liver injury. In contrast, acute knockdown of Parkin had decreased hepatocyte proliferation without or with APAP treatment. Our results suggest that acute and chronic loss of Parkin have different impacts on hepatocyte proliferation and in turn differentially affect APAP-induced liver injury.

Conclusions—In conclusion, Parkin-induced mitophagy is likely a mechanism of protection against APAP-induced liver injury in WT mice because Parkin translocated to mitochon-

dria after APAP treatment. However, Parkin is dispensable for APAP-induced mitophagy in Parkin KO mouse livers. Parkin KO mice may inhibit APAP-induced liver injury by attenuating APAP-induced JNK activation and Mcl-1 degradation while also increasing hepatocyte proliferation. In addition, currently unidentified Parkin-independent mitophagy pathways activated as compensatory and adaptive response during the chronic loss of Parkin likely also play a protective role against APAP-induced liver injury by removing damaged mitochondria. These protective effects in Parkin KO mice were reversed in mice with acute knockdown of Parkin. Therefore, chronic deletion (KO) and acute knockdown of Parkin differentially regulate APAP-induced mitophagy and liver injury in mice. Our results also suggest that caution needs to be exercised for data interpretation when using genetic KO mice for assessing drug-induced liver injury.

Acknowledgments—We acknowledge the Electron Microscopy Research Lab Facility for assistance with the electron microscopy. The EMRL is supported in part by National Institutes of Health COBRE Grant 9P20GM104936. The JEOL JEM-1400 TEM used in the study was purchased with funds from National Institutes of Health Grant S10RR027564. We thank Margitta Lebofsky for technical assistance for the measurement of hepatic GSH.

REFERENCES

1. Larson, A. M. (2007) Acetaminophen hepatotoxicity. *Clin. Liver Dis.* **11,** 525–548
2. McGill, M. R., Sharpe, M. R., Williams, C. D., Taha, M., Curry, S. C., and Jaeschke, H. (2012) The mechanism underlying acetaminophen-induced hepatotoxicity in humans and mice involves mitochondrial damage and nuclear DNA fragmentation. *J. Clin. Invest.* **122,** 1574–1583
3. Ni, H. M., Bockus, A., Boggess, N., Jaeschke, H., and Ding, W. X. (2012) Activation of autophagy protects against acetaminophen-induced hepatotoxicity. *Hepatology* **55,** 222–232
4. Ni, H. M., Williams, J. A., Jaeschke, H., and Ding, W. X. (2013) Zonated induction of autophagy and mitochondrial spheroids limits acetaminophen-induced necrosis in the liver. *Redox Biol.* **1,** 427–432
5. Parzych, K. R., and Klionsky, D. J. (2014) An overview of autophagy: morphology, mechanism, and regulation. *Antioxid. Redox Signal.* **20,** 460–473
6. Reggiori, F., Komatsu, M., Finley, K., and Simonsen, A. (2012) Selective types of autophagy. *Int. J. Cell Biol.* **2012,** 156272
7. Chan, N. C., Salazar, A. M., Pham, A. H., Sweredoski, M. J., Kolawa, N. J., Graham, R. L., Hess, S., and Chan, D. C. (2011) Broad activation of the ubiquitin-proteasome system by Parkin is critical for mitophagy. *Hum Mol. Genet.* **20,** 1726–1737
8. Geisler, S., Holmström, K. M., Skujat, D., Fiesel, F. C., Rothfuss, O. C., Kahle, P. J., and Springer, W. (2010) PINK1/Parkin-mediated mitophagy is dependent on VDAC1 and p62/SQSTM1. *Nat. Cell Biol.* **12,** 119–131
9. Matsuda, N., Sato, S., Shiba, K., Okatsu, K., Saisho, K., Gautier, C. A., Sou, Y. S., Saiki, S., Kawajiri, S., Sato, F., Kimura, M., Komatsu, M., Hattori, N., and Tanaka, K. (2010) PINK1 stabilized by mitochondrial depolarization recruits Parkin to damaged mitochondria and activates latent Parkin for mitophagy. *J. Cell Biol.* **189,** 211–221
10. Narendra, D., Tanaka, A., Suen, D. F., and Youle, R. J. (2008) Parkin is recruited selectively to impaired mitochondria and promotes their autophagy. *J. Cell Biol.* **183,** 795–803
11. Narendra, D. P., Jin, S. M., Tanaka, A., Suen, D. F., Gautier, C. A., Shen, J., Cookson, M. R., and Youle, R. J. (2010) PINK1 is selectively stabilized on impaired mitochondria to activate Parkin. *PLoS Biol.* **8,** e1000298
12. Vives-Bauza, C., Zhou, C., Huang, Y., Cui, M., de Vries, R. L., Kim, J., May, J., Tocilescu, M. A., Liu, W., Ko, H. S., Magrané, J., Moore, D. J., Dawson, V. L., Grailhe, R., Dawson, T. M., *et al.* (2010) PINK1-dependent recruitment of Parkin to mitochondria in mitophagy. *Proc. Natl. Acad. Sci. U.S.A.* **107,** 378–383
13. Kitada, T., Asakawa, S., Hattori, N., Matsumine, H., Yamamura, Y., Minoshima, S., Yokochi, M., Mizuno, Y., and Shimizu, N. (1998) Mutations in the parkin gene cause autosomal recessive juvenile parkinsonism. *Nature* **392,** 605–608
14. Ding, W. X., and Yin, X. M. (2012) Mitophagy: mechanisms, pathophysiological roles, and analysis. *Biol. Chem.* **393,** 547–564
15. Ryan, P. M., Bourdi, M., Korrapati, M. C., Proctor, W. R., Vasquez, R. A., Yee, S. B., Quinn, T. D., Chakraborty, M., and Pohl, L. R. (2012) Endogenous interleukin-4 regulates glutathione synthesis following acetaminophen-induced liver injury in mice. *Chem. Res. Toxicol.* **25,** 83–93
16. Ding, W. X., Ni, H. M., DiFrancesca, D., Stolz, D. B., and Yin, X. M. (2004) Bid-dependent generation of oxygen radicals promotes death receptor activation-induced apoptosis in murine hepatocytes. *Hepatology* **40,** 403–413
17. Ni, H. M., Boggess, N., McGill, M. R., Lebofsky, M., Borude, P., Apte, U., Jaeschke, H., and Ding, W. X. (2012) Liver-specific loss of Atg5 causes persistent activation of Nrf2 and protects against acetaminophen-induced liver injury. *Toxicol. Sci.* **127,** 438–450
18. Jaeschke, H., and Mitchell, J. R. (1990) Use of isolated perfused organs in hypoxia and ischemia/reperfusion oxidant stress. *Methods Enzymol.* **186,** 752–759
19. Williams, J. A., Hou, Y., Ni, H. M., and Ding, W. X. (2013) Role of intracellular calcium in proteasome inhibitor-induced endoplasmic reticulum stress, autophagy, and cell death. *Pharm. Res.* **30,** 2279–2289
20. Narendra, D., Tanaka, A., Suen, D. F., and Youle, R. J. (2009) Parkin-induced mitophagy in the pathogenesis of Parkinson disease. *Autophagy* **5,** 706–708
21. Ding, W. X., Ni, H. M., Li, M., Liao, Y., Chen, X., Stolz, D. B., Dorn, G. W., 2nd, and Yin, X. M. (2010) Nix is critical to two distinct phases of mitophagy, reactive oxygen species-mediated autophagy induction and Parkin-ubiquitin-p62-mediated mitochondrial priming. *J. Biol. Chem.* **285,** 27879–27890
22. McGill, M. R., and Jaeschke, H. (2013) Metabolism and disposition of acetaminophen: recent advances in relation to hepatotoxicity and diagnosis. *Pharm. Res.* **30,** 2174–2187
23. Klionsky, D. J., Abdalla, F. C., Abeliovich, H., Abraham, R. T., Acevedo-Arozena, A., Adeli, K., Agholme, L., Agnello, M., Agostinis, P., Aguirre-Ghiso, J. A., Ahn, H. J., Ait-Mohamed, O., Ait-Si-Ali, S., Akematsu, T., Akira, S., *et al.* (2012) Guidelines for the use and interpretation of assays for monitoring autophagy. *Autophagy* **8,** 445–544
24. Gunawan, B. K., Liu, Z. X., Han, D., Hanawa, N., Gaarde, W. A., and Kaplowitz, N. (2006) c-Jun N-terminal kinase plays a major role in murine acetaminophen hepatotoxicity. *Gastroenterology* **131,** 165–178
25. Hanawa, N., Shinohara, M., Saberi, B., Gaarde, W. A., Han, D., and Kaplowitz, N. (2008) Role of JNK translocation to mitochondria leading to inhibition of mitochondria bioenergetics in acetaminophen-induced liver injury. *J. Biol. Chem.* **283,** 13565–13577
26. Henderson, N. C., Pollock, K. J., Frew, J., Mackinnon, A. C., Flavell, R. A., Davis, R. J., Sethi, T., and Simpson, K. J. (2007) Critical role of c-jun (NH2) terminal kinase in paracetamol-induced acute liver failure. *Gut* **56,** 982–990
27. Saito, C., Lemasters, J. J., and Jaeschke, H. (2010) c-Jun N-terminal kinase modulates oxidant stress and peroxynitrite formation independent of inducible nitric oxide synthase in acetaminophen hepatotoxicity. *Toxicol. Appl. Pharmacol.* **246,** 8–17
28. Sharma, M., Gadang, V., and Jaeschke, A. (2012) Critical role for mixed-lineage kinase 3 in acetaminophen-induced hepatotoxicity. *Mol. Pharmacol.* **82,** 1001–1007
29. Shinohara, M., Ybanez, M. D., Win, S., Than, T. A., Jain, S., Gaarde, W. A., Han, D., and Kaplowitz, N. (2010) Silencing glycogen synthase kinase-3β inhibits acetaminophen hepatotoxicity and attenuates JNK activation and loss of glutamate cysteine ligase and myeloid cell leukemia sequence 1. *J. Biol. Chem.* **285,** 8244–8255
30. Maurer, U., Charvet, C., Wagman, A. S., Dejardin, E., and Green, D. R. (2006) Glycogen synthase kinase-3 regulates mitochondrial outer mem-

brane permeabilization and apoptosis by destabilization of MCL-1. *Mol. Cell* **21,** 749–760
31. Nijhawan, D., Fang, M., Traer, E., Zhong, Q., Gao, W., Du, F., and Wang, X. (2003) Elimination of Mcl-1 is required for the initiation of apoptosis following ultraviolet irradiation. *Genes Dev.* **17,** 1475–1486
32. Fujiwara, M., Marusawa, H., Wang, H. Q., Iwai, A., Ikeuchi, K., Imai, Y., Kataoka, A., Nukina, N., Takahashi, R., and Chiba, T. (2008) Parkin as a tumor suppressor gene for hepatocellular carcinoma. *Oncogene* **27,** 6002–6011
33. Wang, F., Denison, S., Lai, J. P., Philips, L. A., Montoya, D., Kock, N., Schüle, B., Klein, C., Shridhar, V., Roberts, L. R., and Smith, D. I. (2004) Parkin gene alterations in hepatocellular carcinoma. *Genes Chromosomes Cancer* **40,** 85–96
34. Ni, H. M., Du, K., You, M., and Ding, W. X. (2013) Critical role of FoxO3a in alcohol-induced autophagy and hepatotoxicity. *Am. J. Pathol.* **183,** 1815–1825
35. Getachew, Y., James, L., Lee, W. M., Thiele, D. L., and Miller, B. C. (2010) Susceptibility to acetaminophen (APAP) toxicity unexpectedly is decreased during acute viral hepatitis in mice. *Biochem. Pharmacol.* **79,** 1363–1371
36. Piquereau, J., Godin, R., Deschênes, S., Bessi, V. L., Mofarrahi, M., Hussain, S. N., and Burelle, Y. (2013) Protective role of PARK2/Parkin in sepsis-induced cardiac contractile and mitochondrial dysfunction. *Autophagy* **9,** 1837–1851
37. Czaja, M. J., Ding, W. X., Donohue, T. M., Jr., Friedman, S. L., Kim, J. S., Komatsu, M., Lemasters, J. J., Lemoine, A., Lin, J. D., Ou, J. H., Perlmutter, D. H., Randall, G., Ray, R. B., Tsung, A., and Yin, X. M. (2013) Functions of autophagy in normal and diseased liver. *Autophagy* **9,** 1131–1158
38. Lemasters, J. J. (2014) Variants of mitochondrial autophagy: Types 1 and 2 mitophagy and micromitophagy (Type 3). *Redox Biol.* **2,** 749–754
39. Ding, W. X., Guo, F., Ni, H. M., Bockus, A., Manley, S., Stolz, D. B., Eskelinen, E. L., Jaeschke, H., and Yin, X. M. (2012) Parkin and mitofusins reciprocally regulate mitophagy and mitochondrial spheroid formation. *J. Biol. Chem.* **287,** 42379–42388
40. Zhang, H., Bosch-Marce, M., Shimoda, L. A., Tan, Y. S., Baek, J. H., Wesley, J. B., Gonzalez, F. J., and Semenza, G. L. (2008) Mitochondrial autophagy is an HIF-1-dependent adaptive metabolic response to hypoxia. *J. Biol. Chem.* **283,** 10892–10903
41. Liu, L., Feng, D., Chen, G., Chen, M., Zheng, Q., Song, P., Ma, Q., Zhu, C., Wang, R., Qi, W., Huang, L., Xue, P., Li, B., Wang, X., Jin, H., *et al.* (2012) Mitochondrial outer-membrane protein FUNDC1 mediates hypoxia-induced mitophagy in mammalian cells. *Nat. Cell Biol.* **14,** 177–185
42. Zhang, J., and Ney, P. A. (2008) NIX induces mitochondrial autophagy in reticulocytes. *Autophagy* **4,** 354–356
43. Schweers, R. L., Zhang, J., Randall, M. S., Loyd, M. R., Li, W., Dorsey, F. C., Kundu, M., Opferman, J. T., Cleveland, J. L., Miller, J. L., and Ney, P. A. (2007) NIX is required for programmed mitochondrial clearance during reticulocyte maturation. *Proc. Natl. Acad. Sci. U.S.A.* **104,** 19500–19505
44. Sandoval, H., Thiagarajan, P., Dasgupta, S. K., Schumacher, A., Prchal, J. T., Chen, M., and Wang, J. (2008) Essential role for Nix in autophagic maturation of erythroid cells. *Nature* **454,** 232–235
45. Chu, C. T., Ji, J., Dagda, R. K., Jiang, J. F., Tyurina, Y. Y., Kapralov, A. A., Tyurin, V. A., Yanamala, N., Shrivastava, I. H., Mohammadyani, D., Qiang Wang, K. Z., Zhu, J., Klein-Seetharaman, J., Balasubramanian, K., Amoscato, A. A., *et al.* (2013) Cardiolipin externalization to the outer mitochondrial membrane acts as an elimination signal for mitophagy in neuronal cells. *Nat. Cell Biol.* **15,** 1197–1205
46. Chu, C. T., Bayir, H., and Kagan, V. E. (2014) LC3 binds externalized cardiolipin on injured mitochondria to signal mitophagy in neurons: implications for Parkinson disease. *Autophagy* **10,** 376–378
47. Latchoumycandane, C., Goh, C. W., Ong, M. M., and Boelsterli, U. A. (2007) Mitochondrial protection by the JNK inhibitor leflunomide rescues mice from acetaminophen-induced liver injury. *Hepatology* **45,** 412–421
48. Hwang, S., Kim, D., Choi, G., An, S. W., Hong, Y. K., Suh, Y. S., Lee, M. J., and Cho, K. S. (2010) Parkin suppresses c-Jun N-terminal kinase-induced cell death via transcriptional regulation in *Drosophila*. *Mol. Cells* **29,** 575–580
49. Cha, G. H., Kim, S., Park, J., Lee, E., Kim, M., Lee, S. B., Kim, J. M., Chung, J., and Cho, K. S. (2005) Parkin negatively regulates JNK pathway in the dopaminergic neurons of *Drosophila*. *Proc. Natl. Acad. Sci. U.S.A.* **102,** 10345–10350
50. Liu, M., Aneja, R., Sun, X., Xie, S., Wang, H., Wu, X., Dong, J. T., Li, M., Joshi, H. C., and Zhou, J. (2008) Parkin regulates Eg5 expression by Hsp70 ubiquitination-dependent inactivation of c-Jun NH_2-terminal kinase. *J. Biol. Chem.* **283,** 35783–35788
51. Doddareddy, M. R., Rawling, T., and Ammit, A. J. (2012) Targeting mitogen-activated protein kinase phosphatase-1 (MKP-1): structure-based design of MKP-1 inhibitors and upregulators. *Curr. Med. Chem.* **19,** 163–173
52. Dunn, C., Wiltshire, C., MacLaren, A., and Gillespie, D. A. (2002) Molecular mechanism and biological functions of c-Jun N-terminal kinase signalling via the c-Jun transcription factor. *Cell. Signal.* **14,** 585–593
53. Warr, M. R., and Shore, G. C. (2008) Unique biology of Mcl-1: therapeutic opportunities in cancer. *Curr. Mol. Med.* **8,** 138–147
54. Doble, B. W., and Woodgett, J. R. (2003) GSK-3: tricks of the trade for a multi-tasking kinase. *J. Cell Sci.* **116,** 1175–1186
55. Wang, W., Wang, Y. Q., Meng, T., Yi, J. M., Huan, X. J., Ma, L. P., Tong, L. J., Chen, Y., Ding, J., Shen, J. K., and Miao, Z. H. (2014) MCL-1 degradation mediated by JNK activation via MEKK1/TAK1-MKK4 contributes to anticancer activity of new tubulin inhibitor MT189. *Mol. Cancer Ther.* **13,** 1480–1491
56. Ekholm-Reed, S., Goldberg, M. S., Schlossmacher, M. G., and Reed, S. I. (2013) Parkin-dependent degradation of the F-box protein Fbw7β promotes neuronal survival in response to oxidative stress by stabilizing Mcl-1. *Mol. Cell Biol.* **33,** 3627–3643